JOURNAL OF SOLID STATE CHEMISTRY 47, 59–68 (1983)

# Influence of Extended Defects and of the Porous Texture in the Reduction of Chromium Dioxide

R. SÁEZ-PUCHE AND M. A. ALARIO-FRANCO

*Departamento de Química Inorgánica, Facultad de Ciencias Químicas, Universidad Complutense, Madrid 3, Spain, and Instituto de Química Inorgánica "Elhuyar," C.S.I.C. Madrid, Spain*

Received June 1, 1982; and in revised form November 2, 1982

The hydrogen reduction of very small single crystalline particles of $CrO_2$ to orthorhombic CrOOH is impeded by the presence of extended defects, crystallographic shear planes, formed in the process of attaining the reduction temperature in vacuum. However, if $CrO_2$ is predecomposed to a large extent, a porous texture is formed that facilitates the reduction. These results are in full agreement with a previously proposed reaction mechanism based on unidimensional diffusion.

## Introduction

In a series of previous papers (*1–5*) we have studied several aspects of the solid state chemistry of chromium dioxide. In the first of these papers (*1*) we demonstrated the interconversion between $CrO_2$ and orthorhombic CrOOH which was shown to be a topotactic reaction. Subsequently, we analyzed the thermal decomposition of $CrO_2$. Within the context of this process, which can be represented by

$$2CrO_2 \rightarrow Cr_2O_3 + \tfrac{1}{2}O_2 \qquad (1)$$

we have demonstrated the formation of crystallographic shear planes (*2*) and we have analyzed the evolution of the porous texture when chromium dioxide is decomposed in vacuum (*3*) and in air (*4*).

In the latest papers of the series (*5*) we have dealt with the kinetics and mechanistic aspects of the hydrogen reduction of very small crystalline particles of $CrO_2$, according to

$$CrO_2 + \tfrac{1}{2}H_2 \xrightarrow[P_{H_2} = 30\text{–}165\ \text{Torr}]{T = 490\text{–}519\ \text{K}} CrOOH. \qquad (2)$$

It appears from that work (*5*) that such process is diffusion controlled and happens by means of a direct interstitial mechanism in which the hydrogen diffuses along the empty tunnels, parallel to the *c* axis, that exist in the rutile-type structure of $CrO_2$ (*6*). The diffusion equation is of the form

$$D = 10^{-6} \exp(-19.3 \pm 2{,}3/RT)\ \text{cm}^2\ \text{sec}^{-1} \qquad (3)$$

from which it follows that the diffusion coefficient of hydrogen in $CrO_2$, at room temperature, is of the order of $10^{-10}$ $cm^2$ $sec^{-1}$.

It was also observed in the course of this work (*5, 7*) that, for samples with average crystal length $\tau$ smaller than 0.348 $\mu$m, the final reduced state $\alpha_F$ was below 0.75 ($\alpha_F$ = 1 corresponds to total reduction, as in Eq. (2)). Moreover, $\alpha_F$ was smaller the smaller the particle length was. Thus, at $T$ = 514 K and $P_{H_2}$ = 110 Torr, $\alpha_F$ = 0.54 for the sam-



0022-4596/83/040059-10$03.00/0

ple with $\tau = 0.250$ $\mu$m, while $\alpha_F = 0.84$ for the sample with $\tau = 0.431$ $\mu$m ($\tau$ being the average particle length as determined by electron microscopy (*5*)).

The reason of such behavior appears to lie in the incipient decomposition of $CrO_2$ that, inevitably, happens in the process of attaining the reduction temperature in vacuum. For a comparable temperature this decomposition has been observed to be larger the smaller the particle length is (*4*, *7*).

We analyze in this paper the reduction of $CrO_2$ with the smallest particle lengths at our disposal, and we try to correlate all the previously acquired information regarding this interesting system.

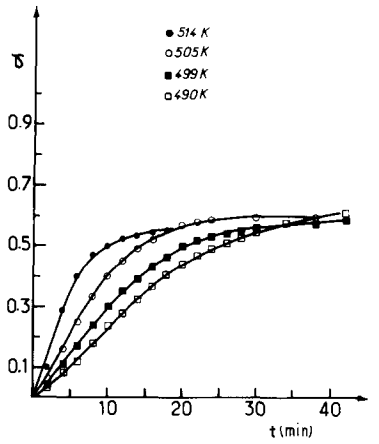


FIG. 1. Reduction isotherms for the sample with $\tau = 0.250$ $\mu$m at $P_{H_2} = 110$ Torr.

## Experimental

The characteristics of the $CrO_2$ powders and the methods used in their study were described in a preceding paper (*5*). The samples of $CrO_2$ were formed by very small, single-crystalline particles with homogeneous prismatic morphology and an acicularity ratio of ~10/1. Samples of different batches were used; their average length $\tau$, as determined by electron microscopy, and their BET areas $S_{BET}$, as measured by nitrogen absorption at its boiling point, were between $\tau = 0.250$ $\mu$m ($S_{BET} = 30.7$ $m^2g^{-1}$) and $\tau = 0.431$ $\mu$m ($S_{BET} = 11.0$ $m^2g^{-1}$).

## Results and Discussion

Figure 1 shows an example of the evolution of the degree of reduction $\alpha$, with the time, at several temperatures and a hydrogen pressure of 110 Torr, for the sample with the smallest average particle length, $\tau = 0.250$ $\mu$m. It is seen that, as expected, the reduction rate increases with the temperature. Nevertheless, all the $\alpha/t$ curves level off for $\alpha > 0.5$. On the other hand, Fig. 2 shows the influence of the particle length on the reduction of $CrO_2$ at fixed temperature, 505 K, and hydrogen pressure, 110 Torr. It can be observed that there is a marked difference between the sample with $\tau = 0.431$ $\mu$m and the other samples with smaller $\tau$ (0.250, 0.304, and 0.314 $\mu$m). For the samples with the smallest particle length, the reduction is faster, but its rate decreases very markedly for $\alpha$ values near 0.5–0.6. On the other hand, the reduction of $CrO_2$ with the longer particle length is clearly slower; nevertheless, its rate is still appreciable for $\alpha$ values in excess of 0.6. In other words, the reduction of the longer particles leads to much higher final reduced states. The differences in rate—i.e., in slope—between the samples with different size could, at a first glance, be attributed to the influence of an interface reaction, since the BET area of, for example, the sample with $\tau = 0.250$ $\mu$m is $S_{BET} = 31$ $m^2g^{-1}$ while for the sample with $\tau = 0.431$ $\mu$m, $S_{BET} = 11$ $m^2g^{-1}$ (see the experimental part, above). However, the difference in the final reduced states of those two samples does not seem to depend on an interface process, but rather to argue against such process.

A general trend for this process is that for the greater particle length a higher final reduced state is obtained. Table I gives the

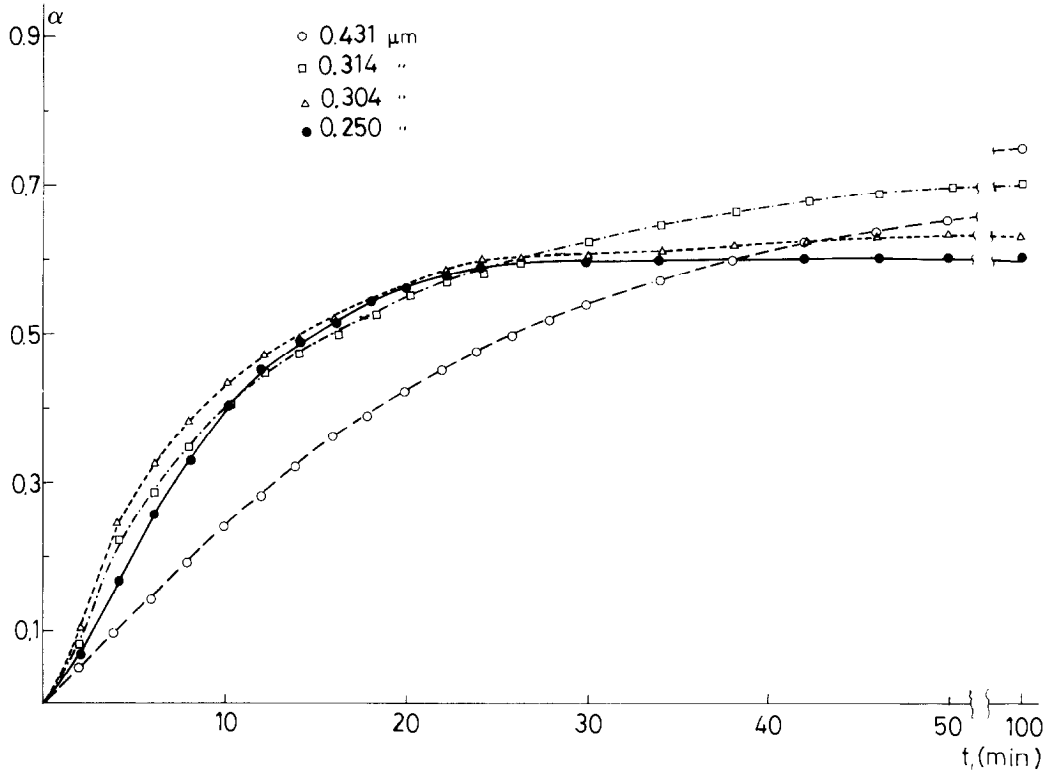


FIG. 2. Influence of the particle dimension, $\tau$, on the reduction of $CrO_2$ at 505 K and $P_{H_2}$ = 110 Torr.

values of the final reduced state $\alpha_F$ and percent decomposition $P_D$ observed before the actual reduction started, at a fixed temperature, 505 K, and a constant hydrogen pressure 110 Torr; the maximum value for $P_D$ is 9.7% as in (1). It can be seen that the smaller the value of $\tau$ the higher is $P_D$ and the smaller is $\alpha_F$.

TABLE I

PREDECOMPOSITION OBSERVED $P_D$ AND FINAL REDUCED STATE $\alpha_F$ ON SAMPLES OF $CrO_2$ WITH DIFFERENT AVERAGE PARTICLE LENGTH $\tau$[a]

| $\tau$ (μm) | $P_D$ (%)[b] | $\alpha_F$[c] |
|---|---|---|
| 0.250 | 0.70 | 0.60 |
| 0.304 | 0.61 | 0.63 |
| 0.314 | 0.41 | 0.71 |
| 0.431 | 0.31 | 0.75 |

[a] Temperature of reduction 505 K. $P_{H_2}$ = 100 Torr.

[b] Maximum value of $P_D$ = 9.7%, Eq. (1).

[c] Maximum value of $\alpha_F$ = 1, Eq. (2).

It is then quite obvious that the reduction of $CrO_2$ depends on the decomposition experienced by the sample, when heated at constant temperature in vacuum up to a constant weight, before introducing the hydrogen in the reaction system. It seems appropriate then to consider here the main characteristics of the thermal decomposition of $CrO_2$.

There are conflicting reports on the temperature at which this decomposition starts; for example, Rodbell and de Vries (*8*) indicated that the most probable temperature of decomposition ($T_D$) in air was 673 K. However, Darnell and Cloud (*9*) cited a much lower temperature of $T_D$ = 523 K. Kubota (*10*) and Roy (*11*) have demon-

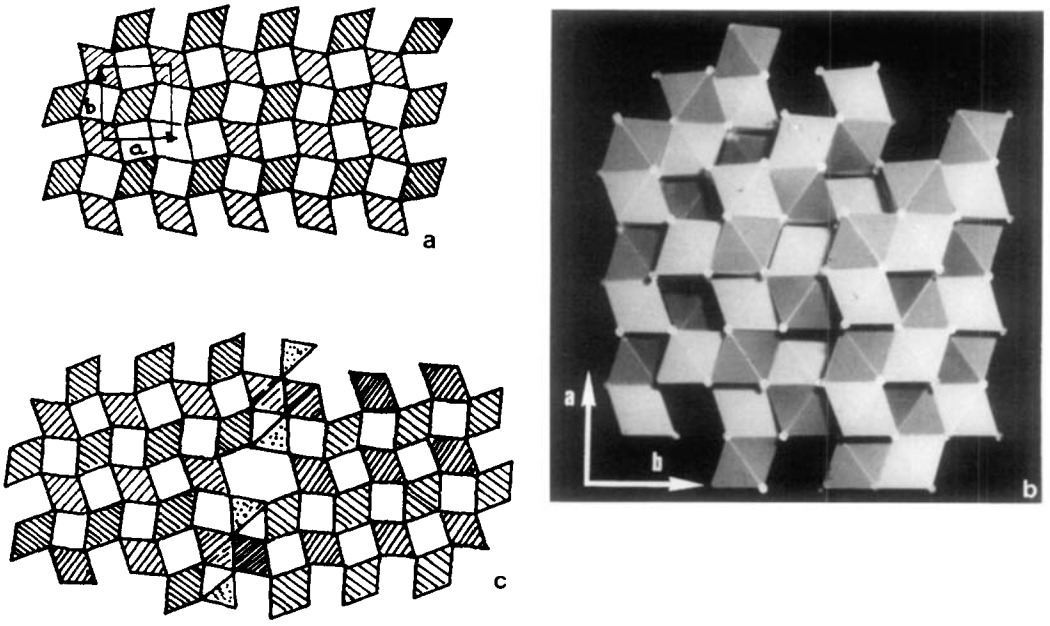


FIG. 3. (a) |001| projection of the rutile structure of $CrO_2$. The empty squares represent the empty columnar tunnels. (b) Perspective |001| view of the a model of the rutile structure showing that the presence of *CS* (121) planes closes up the empty square tunnels. (c) Big hexagonal tunnels and small triangular tunnels produced by *CS* (210) planes in the structure of $CrO_2$.

strated by an analysis of the $Cr-O_2$ phase diagram that this temperature depends on the oxygen pressure. We have observed by thermogravimetry (*7*) that the decomposition in vacuum, $10^{-4}$ Torr, starts at about 473 K—but this figure depends markedly on the particle dimensions. It can be seen in Table I that, for the same temperature and a constant period of time (1 hr), the samples with the smaller particle length decompose to a greater extent than those composed of larger crystals. This fact can be explained by the higher surface area of the former, because this decomposition has been shown to be an interface-controlled reaction (*10, 12*). However, the differences in $\alpha_F$ cannot be explained on such basis.

Another important aspect of the decomposition of $CrO_2$ is the structural one. It has been shown (*2*) that, under certain conditions, the decomposition of $CrO_2$ can take place minimally via two types of crystallographic shear phases: one is a family, of general formula $Cr_nO_{2n-1}$, based on crystallographic shear on the $(121)_R$ oxygen-only planes of the rutile type structure; another is the homologous series with stoichiometry $Cr_mO_{2m-2}$, based on the $(210)_R$ oxygen-only planes (Fig. 3). In considering the possible influence of this *CS* planes on the mechanism of reduction of $CrO_2$ it is important to distinguish between both families since the presence of *CS* $(121)_R$ planes will close up the tunnels parallel to the *c* axis, making an angle of 55.9° to *c* (*13*). This will most likely impede the progress of hydrogen along the tunnels (Fig. 3b). On the other hand, the *CS* $(210)_R$ planes will not disturb the reduction mechanism along *c* since such planes are parallel to *c* (Fig. 3c). In fact, the presence of $(210)_R$ *CS* planes would, if anything, facilitate the hydrogen reduction of the $CrO_2$ comprised between them, since, as can be seen in Fig. 3c, they open up a series of quite large tunnels of hexagonal cross section (*14*).

It would then appear that, if the incipient decomposition of $CrO_2$ were to produce *CS* $(121)_R$ planes, the subsequent reduction with hydrogen would be greatly diminished, or even prevented. With these ideas in mind, we tried to detect such *CS* planes, a task which is not easy with the crystal size that we are using (*15*). X-ray powder diffraction data failed to detect any other phase than $CrO_2$ on the partly decomposed unreduced materials, or other than $CrO_2$ and CrOOH on the reduced samples with $\tau = 0.250$ $\mu$m. However, high-resolution electron microscopy allowed us to detect the presence of ordered *CS* planes in the sample with $\tau = 0.348$ $\mu$m, decomposed for 1 hr at 773 K in air, as shown in Fig. 4a. It can be seen that *CS* $(121)_R$ planes are present with an interplanar distance of $D_{CS} = 7.3$ Å, and making an angle of about 55° with the particle longest dimension, that is, with the *c* axis.

There exists an approximate relation between stoichiometry, as given by *n* in $Cr_nO_{2n-1}$ and the interplanar $D_{CS}$ spacing (*2, 13, 16*), namely,

$$D_{CS} = d_{(121)_R}(n - 0.5), \qquad (4)$$

where $d_{121}$ is the interplanar spacing of the $(121)_R$ planes in $CrO_2 = 1.634$ Å (*6*). From this relation one finds $n = 5$, corresponding to the homologous member $Cr_5O_9$ or $CrO_{1.80}$. This composition is quite close to that expected from the weight loss in such treatment which was $P_D = 5\%$, i.e., $CrO_{1.74}$.

It should be mentioned that the reduction process does not eliminate the *CS* planes. Figure 4b shows that they are still present in two overlapping crystals of the same sample after reduction. It is to be stressed that the X-ray powder diagram of this reduced sample did show the presence of both $CrO_2$ and CrOOH.

It would then appear that the reduction of $CrO_2$ can be diminished by the presence of *CS* planes, in full agreement with the proposed (*5*) direct interstitial mechanism along the empty tunnels parallel to *c*. As the

TABLE II

NUMERICAL DATA FOR THE REDUCTION (AT $P_{H_2} = 110$ TORR) OF PARTLY DECOMPOSED SAMPLES OF $CrO_2$ OF SEVERAL DIFFERENT AVERAGE PARTICLE LENGTHS $\tau$

| RUN N° | $\tau$ ($\mu$m) | $T_D$ (K) | $P_D$ (%) | $T_R$ (K) | $t_{0.5}$ (min) | $\alpha_F$ |
|---|---|---|---|---|---|---|
| 1 | 0.250 | 573 (v) | 1.6 | 500 | 9.8 | 0.84 |
| 2 | | 573 (v) | 1.7 | 497 | 10.8 | 0.84 |
| 3 | | 573 (v) | 1.9 | 480 | 12.8 | 0.94 |
| 4 | | 623 (v) | 2.8 | 494 | 6.4 | 1.0 |
| 5 | | 623 (v) | 3.2 | 497 | D | — |
| 6 | | 623 (v) | 3.7 | 491 | 5.2 | 1.0 |
| 7 | 0.348 | 723(A) + 490(v) | 3.9 | 490 | 21.0 | 1.0 |
| 8 | | 723(A) + 653(v) | 5.5 | 483 | 20.0 | 1.0 |
| 9 | | 723(A) + 673(v) | 5.8 | 487 | 19.2 | 1.0 |
| 10 | | 773 (A) | 7.4 | 485 | 9.0 | 1.0 |
| 11 | | 773 (A) | 7.4 | 490 | 8.2 | 1.0 |
| 12 | | 773 (A) | 7.4 | 495 | 6.6 | 1.0 |
| 13 | 0.362 | 623 (v) | 0.90 | 219 | 5.4 | 1.0 |
| 14 | | 623 (v) | 1.6 | 219 | 4.9 | 1.0 |

*Note.* $T_D$ = Temperature at which $CrO_2$ was partly decomposed, A, in air; v, in vacuum. $P_D$ = % decomposition of each sample at $T_D$; maximum value of $P_D = 9.7\%$, Eq. (1). $T_R$ = Temperature of reduction. $t_{0.5}$ = Half reaction time: time to reach $\alpha = 0.5$. $\alpha_F$ = Expeirmental value of the final reduced state. D = Sample decomposed to $\alpha$-$Cr_2O_3$.

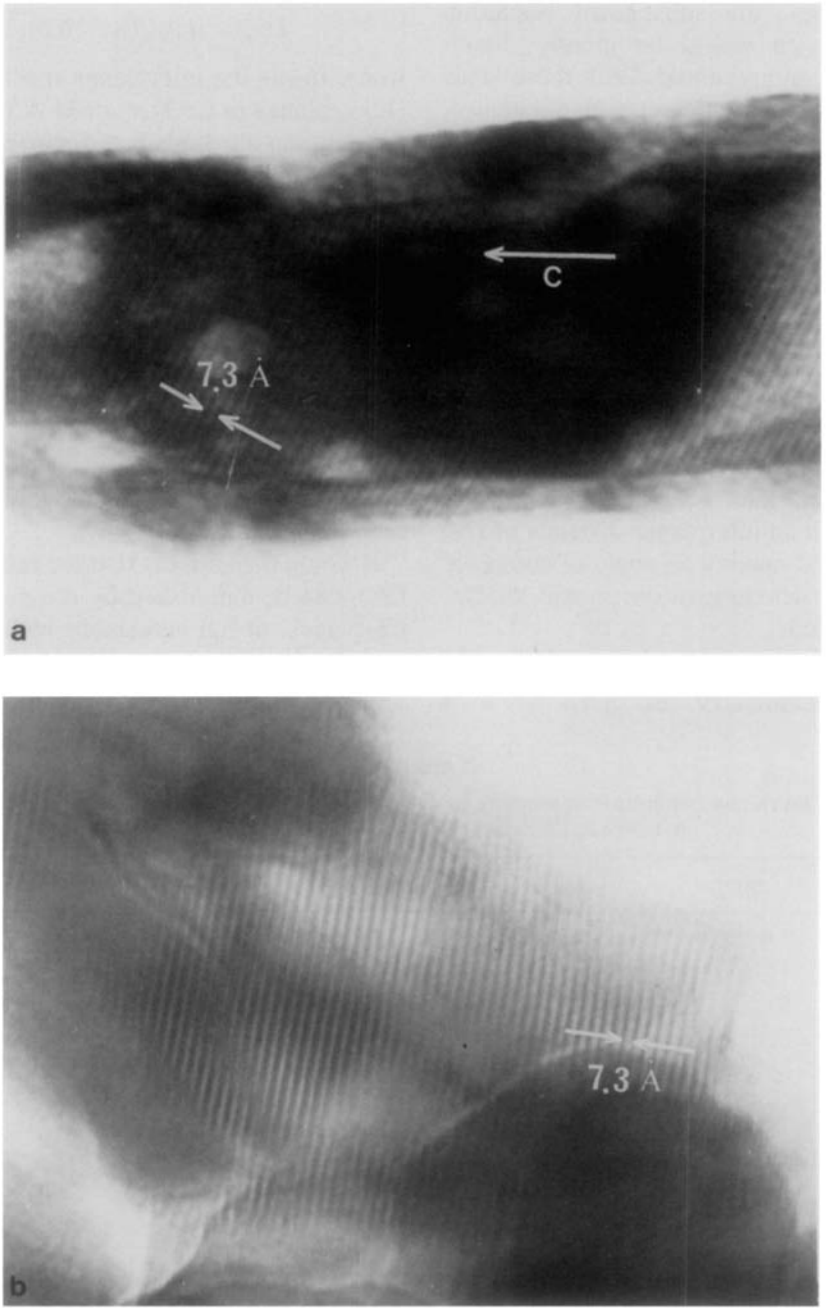


FIG. 4. (a) High-resolution electron micrograph of a single particle of decomposed $CrO_2$ showing ordered *CS* (121) planes. (b) High-resolution electron micrograph of the same sample after reduction at $P_{H_2}$ = 110 Torr and 483 K. The *CS* (121) planes are clearly visible.

smaller samples are more reactive with respect to the decomposition they cannot be completely reduced. It is then easier to reduce totally the samples with larger particle dimensions since, being less reactive towards decomposition, a smaller number of *CS* planes will be produced in the process of attaining the reduction temperature in vacuum.

To check this reasoning, several samples of $CrO_2$ were decomposed, in air and under vacuum, to different controlled values of $P_D$, previous to its reduction. Table II collects the most significant data obtained in their reduction. The $\tau = 0.250$ $\mu$m sample cannot be completely reduced for $P_D < 2\%$; moreover the $t_{0.5}$ values (which represent the time to attain the value $\alpha = 0.5$), indicate that the reaction is slower the greater the initial decomposition within this range is. These results appear to support the idea of the deleterious influence of the *CS* (121) planes on the reduction process. However, for this same sample and for $P_D > 2\%$, as well as for the remaining samples, and for any $P_D$, the value $\alpha_F = 1$ is attained (Table II); moreover, the reduction goes faster, i.e., $t_{0.5}$ is smaller, the greater $P_D$ is. These data contradict the above reasoning.

To sort out the impasse, we have to consider yet another important aspect of the thermal decomposition of $CrO_2$. Our previous work (*3, 4*) on the textural properties of $CrO_2$ indicates that, although all these samples were initially nonporous, a porous texture was formed during the decomposition process. This texture is quantitatively more important when the decomposition is carried out in vacuum (*3, 4, 7*). Under those circumstances, slit-shaped micropores are formed, at about 200°C, when the weight loss is of the order of 2.0%. These pores widen to mesopores when the temperature reaches 450°C and they attain their maximum volume of $10^{-5}$ $m^3$ $Kg^{-1}$ for a $P_D$ value of about 7% at this temperature (*3*). The presence of these pores (Fig. 5a) will allow the hydrogen to reach the tunnels even if these were occasionally interrupted by *CS* $(121)_R$ planes. This seems to explain the increase in reactivity toward hydrogen of the $\tau = 0.250$ $\mu$m sample for $P_D > 2\%$. It may be due to the increase in porosity and may also facilitate the reduction up to $\alpha_F = 1$. In fact, the influence of the porosity produced in the course of the thermal treatment is so marked, that the reduction of a sample which is predecomposed to a greater extent is faster, and attains higher $\alpha_F$ values than the reduction of samples decomposed to a lesser extent even if these are reduced at a higher temperature. One should compare curve *c* ($P_D = 1.9\%$; $T_R = 480$ K) with curve *a* ($P_D = 1.6\%$; $T_R = 500$ K) and curve *d* ($P_D = 2.8\%$; $T_R = 494$ K) with curve *e* ($P_D = 3.7\%$; $T_R = 491$ K), in Fig. 6. Under these circumstances it is not surprising that the data for the reduction of $CrO_2$ with the smaller particle sizes $\tau = 0.250$ $\mu$m and $\tau = 0.304$ $\mu$m did not fit a unidimensional diffusion equation (*7*).

For the case of the samples predecomposed in air (Table II) the situation is somewhat different. In the first instance, the half reaction times are much longer than in the case of the vacuum-treated sample; nevertheless $\alpha_F$ is always unity. This seems to be due to the fact that, in the treatment in air, the pore volume generated for a comparable temperature is only a third of that obtained in vacuum (*4*). The changes in the particle morphology are also different. Instead of slit-shaped micropores, as in Fig. 5a, the $CrO_2$ particles deform (Fig. 5b) and join together in an early stage of the sintering process.

## Summary and Conclusions

The present work shows quite conclusively that what is usually called the "history of a solid" dramatically influences its reactivity; what it demonstrates in more


FIG. 5. (a) Electron micrograph of a $CrO_2$ sample ($\tau$ = 0.250 $\mu$m) showing a slit-shaped micropores formed in the treatment in vacuum at 473 K. (b) Electron micrograph of $CrO_2$ ($\tau$ = 0.348 $\mu$m) treated at 723 K in air showing the change in the morphology of the particles.

concrete terms is that this reactivity is very much dependent on

(a) structure: the reduction of $CrO_2$ being a clear example of a topotactic reaction (*1*).

(b) lattice defects, and in this particular case, extended defects.

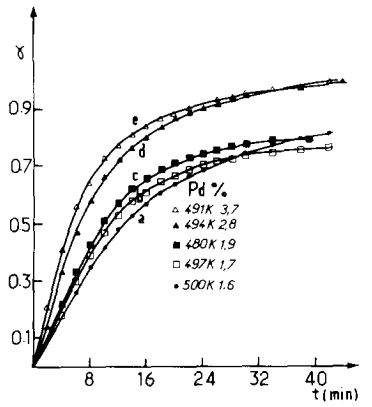


FIG. 6. Influence of the porosity produced in the decomposition of $CrO_2$ at 573 K in its subsequent reduction; $\tau = 0.250$ μm, $P_{H_2} = 110$ Torr.

(c) texture: including such aspects as morphology, particle dimensions, and porosity, which can facilitate the process and also modify the reaction mechanism and kinetics. As shown above, the texture is, in itself, very much dependent on the conditions in which the solid is treated and, in particular, on the surrounding atmosphere.

It appears from our results that the influence of the thermal decomposition of $CrO_2$ in its subsequent reactivity with hydrogen is reflected, at small amounts of decomposition, $P_D < 2\%$, in the formation of *CS* (121) planes that block the empty tunnels parallel to the *c* axis. It is not implied, however, that the *CS* planes develop in all single-crystal particles, since that would totally prevent the reduction along the tunnels. As $CrO_2$ is a metastable material at atmospheric pressure (*11*), it is difficult to control the number of *CS* planes formed in each crystal under a given set of conditions.

For higher degrees of decomposition, $P_D > 2\%$, a porous texture is developed which promotes the reactivity, permitting the attainment of a fully reduced state, $\alpha_F = 1$.

It is perhaps worth stressing the importance of item (b) above, that is, the influence of crystallographic shear planes in the course of a gas–solid reaction. It is quite likely that other examples will be found. It is interesting to mention that Johnson (*17*) observed that abrasian of the rutile surface strongly inhibited the lithium diffusion and this led Huttington and Sullivan (*18*) to suggest that "the dislocations or the stackings faults so produced would choke off the easy interstitial path." However, no direct evidence was provided in support of this hypothesis.

In the light of the above evidence on $CrO_2$, we believe that the influence of CS planes in the diffusion of cations in rutile and in other solids showing the phenomenon of crystallographic shear, such as $WO_3$ (*19*), $MoO_3$ (*20*), etc., is worthy of detailed study.

## Acknowledgment

We thank Dr. J. Muller (Laboratoire de Cristallographie, C.N.R.S., Grenoble) for valuable comments.

## References

1. M. A. ALARIO FRANCO AND K. S. W. SING, *J. Therm. Anal.* **4,** 47 (1972).
2. M. A. ALARIO FRANCO, J. M. THOMAS, AND R. D. SHANNON, *J. Solid State Chem.* **9,** 261 (1974).
3. M. A. ALARIO FRANCO AND K. S. W. SING, *in* "Pore Structure and Properties of Materials," Proceedings of the Int. Symp. Prague (Tchecoslovakia) 1973 (S. Modrý, Ed.), p. B107, Akademia, Prague (1974).
4. R. SÁEZ PUCHE AND M. A. ALARIO FRANCO, *An. Quim.* **76,B,** 229 (1980).
5. R. SÁEZ PUCHE AND M. A. ALARIO FRANCO, *J. Solid State Chem.* **38,** 87 (1981).
6. P. PORTA, M. MAREZIO, J. P. REMEIKA, AND J. D. DERNIER, *Mat. Res. Bull.* **7,** 157 (1972).
7. R. SÁEZ PUCHE, Ph.D., Thesis, Universidad Complutense, Madrid (1979).
8. D. RODBELL AND R. DE VRIES, *Mat. Res. Bull.* **2,** 491 (1967).
9. F. J. DARNELL AND W. H. CLOUD, *Bull. Soc. Chim. France,* 1164 (1965).

*10.* B. KUBOTA, *J. Amer. Ceram. Soc.* **50,** 56 (1967).
*11.* R. ROY, *Bull, Soc. Chim. France,* 1065 (1965).
*12.* R. D. SHANNON, *J. Amer. Ceram. Soc.* **50,** 56 (1967).
*13.* S. ANDERSSON, *Acta Chem. Scand.* **14,** 1161 (1960).
*14.* D. J. LLOYD, I. E. GREY, AND L. A. BURSILL, *Acta Crystallogr. Sect. B* **32,** 1756 (1976).
*15.* J. S. ANDERSON, *in* Specialist Periodical Reports "Surface and Defect Properties of Solids" (M. W. Roberts and J. M. Thomas Eds.), Vol. 1, p. 12, The Chemical Society, London (1972).
*16.* L. A. BURSILL AND B. HYDE, *Prog. Solid State Chem.* **7,** 178 (1972).
*17.* O. W. JOHNSON, *Phys. Rev. A* **136,** 284 (1964).
*18.* H. B. HUTTINGTON AND G. A. SULLIVAN, *Phys. Rev. Lett.* **14,** 177 (1965).
*19.* A. MAGNELI, *Arkiv. Kemi* **1,** 513 (1950).
*20.* B. BLOMBERG, L. KHILBORG, AND A. MAGNELI, *Arkiv Kemi* **6,** 133 (1953).